Title

Identification of Factors Complicating Bioluminescence Imaging

Journal

Biochemistry, 58(12)

ISSN

0006-2960

Authors

Yeh, Hsien-Wei
Wu, Tianchen
Chen, Minghai
et al.

Publication Date

2019-03-26

DOI

10.1021/acs.biochem.8b01303

Peer reviewed

HHS Public Access

Author manuscript

Biochemistry. Author manuscript; available in PMC 2020 March 26.

Published in final edited form as:

Biochemistry. 2019 March 26; 58(12): 1689–1697. doi:10.1021/acs.biochem.8b01303.

Identification of Factors Complicating Bioluminescence Imaging

Hsien-Wei Yeh, **Tianchen Wu**, **Minghai Chen**, and **Hui-wang Ai***

Center for Membrane and Cell Physiology, Department of Molecular Physiology and Biological Physics, Department of Chemistry, and the UVA Cancer Center, University of Virginia, 1340 Jefferson Park Avenue, Charlottesville, Virginia 22908, United States of America

Abstract

In vivo bioluminescence imaging (BLI) has become a standard, non-invasive imaging modality for following gene expression or the fate of proteins and cells in living animals. Currently, bioluminescent reporters used in laboratories are mostly derivatives of two major luciferase families: ATP-dependent insect luciferases and ATP-independent marine luciferases. Inconsistent results have been reported for experiments using different bioluminescent reporters, such as Akaluc and Antareas2. Herein, we re-examined the inconsistency in several experimental settings and identified that factors, such as ATP dependency, stability in serum, and molecular sizes of luciferases, contributed to the observed differences. We expect this study will make the research community aware of these factors and facilitate more accurate interpretation of BLI data by considering the nature of each bioluminescent reporter.

Graphical Abstract

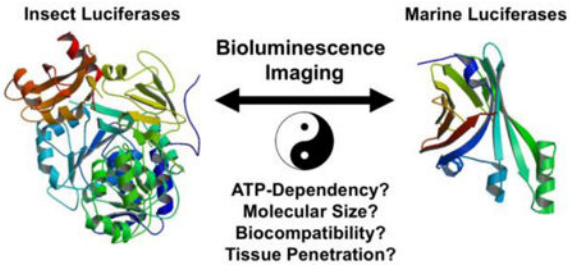

INTRODUCTION

Complementary to magnetic resonance imaging (MRI) and positron-emission tomography (PET), *in vivo* bioluminescence imaging (BLI) offers an accessible and cost-effective method for monitoring gene expression, tumor growth, and protein distribution in animal

*Corresponding Author. huiwang.ai@virginia.edu.

ASSOCIATED CONTENT

Supporting Information

Supplementary figures, including additional bioluminescence and fluorescence characterization data.

Notes

H.w.A. and H.W.Y. are coinventors of a patent filed by the Regents of the University of California, titled “Red-Shifted Luciferase-Luciferin Pairs for Enhanced Bioluminescence”. The sequences of teLuc, Antares2, and Akaluc can be accessed from NCBI GenBank under accession numbers KX963378, KY474379, and LC320664.

models.[1–3] BLI has grown tremendously in the past two decades and become a standard noninvasive and quantitative imaging modality that can provide detailed, time-lapse information on activities and dynamics in animal models without killing animals at various intermediate time points.

Bioluminescent reporters widely used in laboratories can be categorized into two major groups.[4] The first group is mostly derived from insects, such as luciferases from *Photinus pyralis* firefly (FLuc) and click beetles. These enzymes generate light *via* a two-step, oxidative biochemical reaction (Figure 1A). The substrate, D-luciferin, is first adenylated by adenosine triphosphate (ATP) to generate an adenosine monophosphate (AMP)-luciferin intermediate, and subsequently oxidized by molecular oxygen (O_2) to yield excited-state oxyluciferin from which photons with a wavelength of ~ 560 nm are emitted.[5] The second group comprises ATP-independent luciferases that are cloned from luminous marine organisms.[6] Coelenterazine (CTZ) is a shared luciferin for a large number of marine luciferases, such as luciferases from *Renilla reniformis* (RLuc),[7] *Oplophorus gracilirostris* (OLuc),[8] and *Gaussia princeps* (GLuc).[9] In the presence of these marine luciferases, CTZ reacts with O_2 to form a dioxetanone intermediate, which loses CO_2 to give a high-energy, excited-state coelenteramide (Figure 1B). Subsequently, photons at ~ 480 nm are emitted.[10]

FLuc and D-luciferin have been widely utilized for *in vivo* BLI, because its long-wavelength emission is less absorbed and less scattered by mammalian tissue. In recent years, derivatives of FLuc and D-luciferin have been developed and some have generated brighter and even more red-shifted emission. Notably, in early 2018, Iwano *et al.* described an engineered luciferase-luciferin pair, namely Akaluc-AkaLumine, emitting light in the near-infrared (NIR) region for highly sensitive *in vivo* deep-tissue BLI (Figure 2A).[11]

Conventionally, marine luciferases have limited uses for *in vivo* BLI, because blue photons strongly interact with mammalian tissue, leading to poor light penetration. The recent development of marine luciferase derivatives (*e.g.*, NanoLuc and GLuc[12,13]) that produce two orders of magnitude higher photon flux than FLuc has spurred interest in exploring these reporters for *in vivo* BLI. In subcutaneous tumor models,[12,14] the bioluminescence signal from NanoLuc is comparable to FLuc, despite that FLuc still surpassed NanoLuc for deep-tissue imaging.[15] Recently, our lab engineered NanoLuc into teLuc, which emits teal photos in the presence of a synthetic diphenylterazine (DTZ) substrate (Figure 2B).[16] Moreover, further red-shifted emission has been achieved by fusing NanoLuc or teLuc with fluorescent proteins for bioluminescence resonance energy transfer (BRET).[16–19] These studies have partially fulfilled the increasing demand of using the same reporters for *in vitro* and *in vivo*, fluorescence- and bioluminescence-based assays. In particular, the Antares2-DTZ pair was able to produce ~10-fold more detectable bioluminescence than FLuc at the standard D-luciferin concentration in a deep-tissue transfection mouse model.[16]

Some researchers have concerns on whether marine luciferase could be used for *in vivo* BLI, because CTZ and its analogs have high internal energies and are prone to oxidation. [20–22] In a recent report, the Akaluc-AkaLumine pair was compared with Antares2-DTZ by intravenously (i.v.) injecting Akaluc- or Antares2-expressing HeLa cells into mice via tail vain and further intraperitoneally (i.p.) injecting the corresponding substrates before image

acquisition.[11] The signals from Akaluc-AkaLumine were concentrated to lungs. In contrast, the signals from Antares2-DTZ were stronger but more diffuse than Akaluc-AkaLumine. Subsequently, the diffuse signals from Antares2-DTZ were interpreted as background caused by the auto-oxidation of DTZ. This interpretation is in conflict with our previous observation that direct injection of DTZ into blank mice caused negligible signals, in addition to a plethora of publications which successfully used CTZ or CTZ analogs for *in vivo* BLI. [18,23–26]

In this manuscript, we re-investigated the performance of Akaluc and Antares2 bioluminescent reporters for tracking i.v.-injected cells in mice, and by using hydrodynamic transfection and xenograft tumor mouse models. We identified several factors, such as ATP dependency, stability in serum, and molecular size, which significantly affected BLI results. Our data show that although cautions should be made to maintain the *in vitro* stability of DTZ, background bioluminescence is usually not an issue for its *in vivo* applications. Moreover, our results suggest that it is important to consider the properties of each bioluminescent reporter when interpreting BLI results.

EXPERIMENTAL DETAILS

Mammalian cell culture and transfection.

HEK 293T cells were cultured at 37 °C with 5% CO_2 in Dulbecco's Modified Eagle's Medium (DMEM) supplemented with 10% fetal bovine serum (FBS). Transfection mixtures were prepared with 3 μg of plasmid DNA and 9 μg of PEI (polyethylenimine, linear, MW 25 kDa) in DMEM and incubated for 20 min at room temperature. After removing cell culture media, transfection mixtures were added to cells at ~ 70% confluency on 35-mm culture dishes seeded 1 d before transfection. Incubation lasted for 3 h at 37 °C. Fresh DMEM containing 10% FBS was used to replace the transfection mixtures. Cells were cultured at 37 °C in a CO_2 incubator for another 24 h before use.

Bioluminescence imaging of i.v. injected HEK 293T cells.

BALB/c, NU/J and B6 albino mice were obtained from the Jackson Laboratory (Cat. No. 000651, 002019 and 000058). Animals were maintained and treated in standard conditions that complied with all relevant ethical regulations. All animal procedures were approved by the UVA Institutional Animal Care and Use Committee. HEK 293T cells expressing teLuc, Antares2, or Akaluc were trypsinized, pelleted, and re-suspended in 100 μL PBS. Cell numbers were determined using a hemocytometer. 20000 cells were injected into mice placed in a restrainer via tail vein. Mice were allowed to recover. Bioluminescence images were taken at 1h, 5h, and 24h post injection of cells. Mice anaesthetized using isoflurane were i.p. or i.v. injected with 0.3 μmol DTZ in a 100 μL solution containing 8% glycerol, 10% ethanol, 10% hydroxypropyl-β-cyclodextrin, and 35% PEG 400 in water or 1.5 μmol AkaLumine-HCl in 100 μL saline. The 0.3 μmol DTZ solution was each time made fresh from a DTZ (50 mM) stock solution in 1:1 (v/v) EtOH and propylene glycol containing 10 mM HCl (stored at −80°C). Mice under isoflurane anesthesia on a heat pad were next immediately imaged with a Caliper IVIS Spectrum over a course of 20 min. The following conditions were used for image acquisition: open filter for total bioluminescence, exposure

time = 10 s, binning = small, field of view = 21.6 × 21.6 cm, and f/stop = 1. Image analysis was performed using the Living Image 4.3 software. After imaging at each time point, one mouse in each group was sacrificed. Organs were harvest and plated on a petri dish and bioluminescence images were acquired immediately with 1-s exposure. Blood and urine samples were collected for further evaluation.

Bioluminescence assays of blood and urine.

After collection, blood was left to clot at room temperature for 30 min. Clots were removed by centrifugation at 2000×g for 10 min. The resultant supernatant (a.k.a. serum) was store at −80°C. 5 μL of urine or serum was diluted in 100 μL PBS to a white 96-well plates (Costar 3912). 100 μL of DTZ was added to a final concentration of 25 μM. Bioluminescence activities were immediately measured on a Synergy Mx Microplate Reader (BioTek). The following conditions were used for acquisition: open filter, exposure time = 0.1 s, and sensitivity = 130 for teLuc and Antares2; sensitivity =200 for Akaluc. To monitor Akaluc activity in serum or urine, the final concentration of AkaLumine-HCl was at 100 μM. Moreover, 5 mM ATP and 5 mM $MgSO_4$ were supplemented as needed.

Fluorescence imaging of ATP in HEK 293T cells.

HEK 293T cells were cultured and transfected as aforementioned.[16] Images were acquired on a Leica DMi8 inverted microscope equipped with the SPE confocal module. Cells were cultured in DMEM (no phenol red) with 4.5 g/mL glucose. A 488 nm laser was used to excite PercevalHR and emission was collected from 510 nm to 600 nm. Intervals between each image were 5 second. 1 mM D-luciferin or 50 μM DTZ was added to cells. For internal calibration, iodoacetic acid (IAA) was added to a final concentration of 5 mM after D-luciferin to completely deplete ATP.[27]

Hydrodynamic transfection of BALB/c mice.

20 μg of each luciferase-expressing plasmid in 2 mL sterilized saline was injected into restrained mice via tail vein over 8 s. Mice were allowed to recover and monitored until their breathing rate returned to normal. BLI was performed 10 and 48 h post transfection.

NU/J xenograft model.

HeLa cells stably expressing luciferases were dissociated with trypsin and re-suspended in 10 mL DMEM. Cell numbers were determined using a hemocytometer, and cell viability was determined using a trypan blue exclusion test. 10^4 or 10^5 cells were re-suspended in 100 μL FBS-free DMEM containing 50% Matrigel matrix (Corning). 8-week-old female nude mice were first anesthetized using isoflurane. Cells were subcutaneously injected into the left and right dorsolateral trapezius regions or thoracolumbar regions. Mice were recovered on heat pads for 5 min while cells were allowed to settle. BLI were performed on day 5 post cancer cell inoculation.

RESULTS

DTZ in blank mice generated only low background

We first evaluated bioluminescence background in triplicate by injecting 0.3 μmol of DTZ to BALB/c blank mice that received 2×10^4 untransfected human embryonic kidney (HEK) 293T cells via tail vein. Similar to our previous observation for i.p. injection of DTZ,[16] the background signal from i.v. injection was also low (Figure 3). The i.v. and i.p injection of DTZ increased background signals from the instrument noise by 35% and 192%, respectively (Figure S1, Supporting Information). However, these intensities were still about 50-fold less than mice injected with luciferase-labeled HEK 293T cells (see below). To confirm that this background level is not strain-specific, we further injected DTZ into B6 albino mice and similar results were observed (Figure 3). Our data collectively suggest that luminescence background from *in vivo* auto-oxidation of DTZ is low and should not be an issue for typical BLI applications.

Injection of luciferase-labeled cells into mice released the luciferase into blood

We next examined the bioluminescence of BALB/c mice at 1, 5, and 24 h after i.v. injection of 2×10^4 HEK 293T transiently expressing Akaluc, teLuc, or Antares2. After i.v. delivery of AkaLumine, we observed bioluminescence signals of Akaluc from the lung area (Figure 4A). This result agrees with previous studies.[11] In contrast, the signals from teLuc-DTZ were diffuse with peak intensities around the bladder area; the signals from Antares2-DTZ were spread over the entire animals (Figure 4A). Signals from all groups were completely cleared one day after injection of cells to these immunocompetent mice.

We further performed BLI after i.p. delivery of corresponding luciferins (Figure 4B). The Akaluc-AkaLumine group had signals in the lung area, similar to the result post i.v. administration of the substrate. Signals for the teLuc-DTZ group and the Antares2-DTZ group were diffuse with peak intensities around the abdomen region.

To further examine the signal distribution, mice from each group were sacrificed and their organs were immediately extracted. *Ex vivo* BLI of representative organs showed that that bioluminescence from teLuc-DTZ or Antares2-DTZ were detectable in many organs, whereas bioluminescence for Akaluc-AkaLumine was only observed in lungs (Figure 4C and Figure S2). In particular, strong luminescence was detected from the bladders of mice in the teLuc-DTZ group.

We next collected mouse serum and urine samples for *in vitro* bioluminescence assays. We detected strong teLuc or Antares2 activities from the serum of corresponding mice (Figure 5). Moreover, we observed strong bioluminescence from the urine of mice injected with teLuc-labeled HEK 293T cells. These results suggest that teLuc and Antares2 are released into blood after i.v. injection of their labeled mammalian cells into BALB/c mice. Furthermore, likely due to different molecular sizes, teLuc (19 kDa), but not Antares2 (70.5 kDa), can be excreted into urine via renal filtration.

We could not detect much bioluminescence directly from the serum and urine samples of mice injected with Akaluc-labeled HEK 293T cells. Since Akaluc is an ATP-dependent

luciferase, we next supplemented the samples with 5 mM ATP. In the presence of ATP, bioluminescence was unambiguously detected from the serum, suggesting that Akaluc was also released into blood post i.v. injection of the cells.

In addition to low ATP levels, serum further deactivated Akaluc

The serum bioluminescence of mice in the Akaluc-AkaLumine group was much lower than that of mice in the teLuc-DTZ and Antares2-DTZ groups. This could be explained by the fact that Akaluc is ATP-dependent and that the intrinsic photon flux of Akaluc-AkaLumine is lower than that of teLuc-DTZ or Antares2-DTZ.[11] To further investigate whether there are other factors, we mixed recombinant teLuc, Antares2, and Akaluc proteins with serum isolated from untreated blank mice and examined luciferase activities in relation to assays in PBS. For the teLuc and Antares2 groups, the total signals in either serum or PBS within the first 10 min post substrate injection were almost identical (Figure 6A), despite that teLuc and Antares2 displayed a flash-type kinetics in PBS but a sustained light output in serum (Figure S3A). In contrast, Akaluc in serum generated very weak bioluminescence, which could be rescued by ~ 4-fold after addition of 5 mM ATP, but still ~ 16-fold lower than its intensity in PBS (Figures 6B and S3B). These data suggest that, in addition to low ATP levels, mouse serum can further deactivate Akaluc. Serum also deactivated FLuc, as shown in similar experiments (Figures S3C and 3D).

ATP-dependent bioluminescent reporters reduced cellular ATP:ADP

Because ATP-dependent luciferases consume ATP to generate bioluminescence, we sought to determine whether these luciferases impact cellular ATP:ADP levels. We expressed PercevalHR, a previously reported fluorescent ATP/ADP biosensor,[27] in live HEK 293T cells. PercevalHR is an excitation-ratiometric, green fluorescent biosensor with two distinct excitation peaks at ~ 420 and ~ 500 nm. ATP binding increases the excitation of PercevalHR at 500 nm and decreases its excitation at 420 nm.

To our surprise, addition of AkaLumine to mammalian cells generated strong fluorescence as AkaLumine itself is only weakly fluorescent (Figure S4). There was obvious, cell-induced fluorescence activation and the resultant fluorescence seemed to accumulate in intracellular vesicles (Figure S4). The resultant fluorescent species could be excited with both 405 and 488 nm lasers. Similar phenomena were observed in all tested cell lines, including HeLa, HEK 293T, and SH-SY5Y, and does not require corresponding luciferases since fluorescence was also observed for untransfected cells. Moreover, this fluorescent species seemed to act as an effective photosensitizer because AkaLumine-treated cells, when imaged with 488 nm light, underwent morphological changes, including the blebbing of cell membrane and the formation of extracellular vesicles (Figure S5). Due to these reasons, we were unable to use PercevalHR to measure ATP:ADP ratios in AkaLumine-treated cells.

D-Luciferin is highly fluorescent under 405 nm excitation, but not under 488 nm excitation (Figure S4). We thus monitored PercevalHR fluorescence with 488 nm excitation and determined ATP level changes in FLuc-expressing HEK 293T cells in response to addition of D-Luciferin by following a previously reported calibration method.[27] Within a few minutes, the bioluminescence reaction of FLuc-D-luciferin reduced the green fluorescence of

PercevalHR, corresponding to a cellular ATP:ADP ratio change from > 40:1 to ~ 20:1 (Figures 7). D-luciferin itself did not cause any PercevalHR fluorescence change (Figure S6A). Also, the bioluminescence reaction of FLuc-D-luciferin did not affect intracellular pH as monitored by pHRFP, a red fluorescent pH biosensor (Figure S6B).[28]

It is worthwhile to note that DTZ does not induce fluorescence in live cells. Moreover, we observed no ATP perturbation from DTZ-treated, teLuc-expressing cells.

Luciferase was also in the blood of hydrodynamically transfected mice

Hydrodynamic transfection is a systematic gene delivery method.[29] By rapidly injecting a large volume of DNA to mice via tail vein, this method can lead to transient, high-level gene expression in internal organs, including the liver. Previous studies used FLuc and green fluorescent protein (GFP) to examine the distribution of protein expression after hydrodynamic transfection.[30] We re-investigated this using mice hydrodynamically transfected with Antares2 (Figure 8), which is active in blood. At 10 h after plasmid injection, we observed strong bioluminescence in the abdomen region. We retrieved blood from these mice and detected strong luciferase activity in blood. At 48 h, the bioluminescence became more focused around the liver area, likely due to the activity of Antares2 localized in the liver. The data suggest that after hydrodynamic transfection, proteins encoded by delivered genes are transiently detectable in blood.

Luciferases from both families can highlight tumors

BLI has been an important preclinical tool to evaluate the efficacy of a specific treatment by monitor the growth of tumor burden in xenograft models.[3,31] We established HeLa cells that stably express teLuc, Antares2, or Akaluc, and subcutaneously injected 10^4 or 10^5 cells to the left or right dorsolateral trapezius and thoracolumbar regions of NU/J mice. BLI was performed on day 5 after either i.v. or i.p. administration of corresponding luciferins. On-site implantation of luciferase-expressing tumors gave localized and focused bioluminescence signals no matter ATP-dependent or ATP-independent luciferases were used (Figure 9A). After i.v. administration of the corresponding substrates, the signals for Antares2 were comparable to Akaluc. In addition, we observed ~ 3-fold higher bioluminescence after i.v. administration of DTZ compared to i.p. administration. Moreover, Antares2-DTZ showed better sensitivity than teLuc-DTZ, likely due to its red-shifted emission. Delivery of AkaLumine to Akaluc-expressing tumor xenograft mice via i.v. also yielded higher brightness than i.p. administration, but the difference was within ~ 30% (Figure 9B).

DISCUSSION

In this study, we first investigated reasons for different bioluminescence distributions in mice post injection of luciferase-labeled mammalian cells. Our data collectively support that luciferases were released into blood during or after i.v. injection of luciferase-expressing mammalian cells, resulting in diffuse bioluminescence signals from teLuc-DTZ and Antares2-DTZ. We did not observe diffuse bioluminescence signals for Akaluc-AkaLumine, because Akaluc is inactive in blood. It is reasonable to assume that some of i.v. injected cells were trapped in lungs,[32] but some were either lysed during injection or subsequently broken

down by the immune systems of mice. In fact, a few previous studies reported the detection of systemically delivered cells (or in fact their signal labels) in organs other than the lung, [33–38] corroborating our observations.

When mice were injected with teLuc-labeled cells, the accumulation of teLuc in the bladder suggests that the small size of teLuc makes it permeable to the glomerular basement membrane.[39] teLuc accumulated in urine still remained enzymatically active. Bioluminescence was detected in blood, urine, and many internal organs, but the bladder area showed the strongest signals likely because of high concentrations of teLuc in urine and the relatively shallow position of the bladder compared to other internal organs. Bioluminescence is attenuated approximately by a factor of 10 for every centimeter depth of tissue.[40]

For mice injected with Antarea2-labeled cells, signals were observed around the whole body. After sacrificing these mice, bioluminescence was also detectable in blood and many internal organs. The emission of Antarea2 is red-shifted from teLuc and long-wavelength photons are less absorbed and scattered by mammalian tissue. Not surprising, the signals after injection of Antarea2-labeled cells were more diffuse than the signals after injection of teLuc-labeled cells.

ATP-dependent luciferases, such as Akaluc and FLuc, are inactive in blood because of relatively low ATP levels in the extracellular space. Moreover, serum further deactivates Akaluc and FLuc, although the exact mechanism remains to be elucidated. Only signals from the lung were observed for mice injected with Akaluc-labeled cells, because the lung trapped live mammalian cells, which can produce ATP to support the bioluminescence reaction of Akaluc. In contrast, dead cells or Akaluc released in the circulation systems were not detectable when whole mice were imaged.

Although ATP-dependent luciferases, such as FLuc, have been routinely used, their impact on cellular ATP levels has not yet carefully characterized. Assuming the bioluminescence quantum yield is 0.4,[41] to produce each photon, 2.5 ATP molecules are consumed. This is a significant metabolic burden, considering that the luciferases may reach micromolar concentrations in live cells. Despite that live cells can adjust their metabolic network to compensate this bioluminescence-induced metabolic need, we, by co-expressing PercevalHR, a fluorescent biosensor for cellular ATP:ADP ratios, with FLuc, still observed the decrease of intracellular ATP:ADP from > 40:1 to ~ 20:1 during the bioluminescence reaction between FLuc and D-luciferin. We want to note that the dynamic range of PercevalHR is limited to the ATP:ADP ratios of 40:1 to 0.4:1.[27] Previous studies, which used a diverse array of analytical strategies, have reported a wide range of ATP:ADP from 1 to >100 in healthy cells.[27,42–44] Some studies even suggested that ATP:ADP could be up to 200,[45–47] which is way beyond our measurable range. Nevertheless, similar to the previous report,[27] we observed that PercevalHR was saturated under untreated conditions, suggesting that the basal ATP:ADP level is >40 in these cells. The physiological consequence of the metabolic disruption by ATP-dependent luciferases remains to be further investigated. Moreover, because the ATP level is a variable in biological systems and the availability of

ATP may sometimes become a limiting factor, ATP-dependent bioluminescence systems may actually report the co-exist of ATP, the substrate, and the luciferase.

ATP-independent luciferases, such as teLuc and Antares2, can overcome the ATP-dependency issue of ATP-dependent luciferases. However, current ATP-independent bioluminescence systems have a different set of caveats.

First, despite that the luminescence background caused by DTZ auto-oxidation is low and not a problem for most applications, the background might become an issue for detection of very low signals, such as bioluminescence from single cells. We suggest that researchers should always include suitable controls for their particular experiments to exclude autoluminescence. Also, we envision that future research may lead to new CTZ and DTZ analogs to greatly enhance their stability and reduce their auto-oxidation, thereby broadening the application boundary of marine luciferases.

Second, DTZ and its analogs have a delayed biodistribution, as demonstrated by us (Figures 4A, 4B, and 9B) and others.[48,49] The route of administration may have to be optimized for each type of experiments.[24,50] In our xenograft tumor model, i.v. administration was clearly more effective than i.p. delivery of the substrate. We want to note that AkaLumine seemed to be accumulated in the liver, likely for its clearance, as shown by our near-infrared (NIR) fluorescence imaging of organs of AkaLumine-injected mice (Figure S7).

Moreover, DTZ and its analogs have relatively poor water solubility, resulting in limited *in vivo* delivery dosages. Although these ATP-independent luciferases can generate much higher photo flux than FLuc and Akaluc *in vitro*, their brightness *in vivo* is compromised by the low accessibility of substrates and their relatively short-wavelength emission (see below). We expect that further chemical modifications of DTZ and its analogs will improve their water-solubility, biocompatibility, and biodistribution.

Furthermore, the emission of marine luciferase derivatives is less red-shifted than the emission of FLuc or Akaluc, leading to lower tissue penetration. In particular, the depth and opacity of the tissues will complicate signal acquisition and data interpretation. Signals from superficial targets may dominate signals from deep tissue. Also, because BLI is intrinsically a two-dimensional imaging modality, light transmission is dependent of mouse strains. For example, the interaction of light with black mice, albino mice, or hairless mice should be very different.[51] Because of these reasons, we recommend the capturing of bioluminescence on both ventral and dorsal sides. Moreover, further studies are definitely needed to continuously red-shift the emission of marine luciferase derivatives.

In this study, we also investigated hydrodynamic transfection of mice with Antares2. We detected high bioluminescence in blood. It has been reported that high intravascular pressure can stretch the structure of hepatocytes, and subsequently lead to whole-body re-distribution of injected plasmids.[52] This disruption seemed to be effective in releasing of newly synthesized Antares2 to blood. Previous studies used FLuc and GFP as the reporters to study gene expression across various organs, but FLuc and GFP were unable to provide information on gene expression in blood.[30] Therefore, ATP-independent Antares2 provides an alternative insight to this process.

We further demonstrated that both ATP-dependent Akaluc and ATP-independent Antares2 could be used to detect xenograft tumors. Bioluminescence signals were observed at sites for tumor implantation. This experiment was not meant to compare Akaluc and Antares2 for sensitivity, but the result strongly supports that ATP-independent Antares2 does not have intrinsic tendency to generate diffuse signals. Antares2 caused diffuse signals in some systematic delivery experiments, only because the luciferase indeed entered and were still active in body fluids.

In summary, we have identified several key issues impacting the interpretation of BLI results using common ATP-dependent and ATP-dependent bioluminescent reporters. Because of the ATP-independency of Antares2, we expect it may complement ATP-dependent luciferases, such as FLuc and Akaluc, and may reveal new biological insights not detectable with ATP-dependent luciferases. In addition, we envision the possible use of dual BLI with both ATP-dependent and ATP-independent luciferases, not only for tracking multiple targets, but also for factual reporting of a single biological process by breaking natural limitations (*e.g.*, substrate biodistribution, light attenuation by tissue, and ATP availability) of a single bioluminescence system.

Supplementary Material

Refer to Web version on PubMed Central for supplementary material.

ACKNOWLEDGMENT

Research reported in this publication was supported in part by the National Institute of General Medical Sciences of the National Institutes of Health under Awards R01GM118675 and R01GM129291. The content is solely the responsibility of the authors and does not necessarily represent the official views of the National Institutes of Health.

ABBREVIATIONS

BLI	bioluminescence imaging
MRI	magnetic resonance imaging
PET	positron-emission tomography
FLuc	firefly luciferase
BRET	bioluminescence resonance energy transfer
GFP	green fluorescent protein

REFERENCES

(1). Mezzanotte L, van ‘t Root M, Karatas H, Goun EA, and Lowik C (2017) In Vivo Molecular Bioluminescence Imaging: New Tools and Applications, Trends Biotechnol 35, 640–652. [PubMed: 28501458]

(2). Yao Z, Zhang BS, and Prescher JA (2018) Advances in bioluminescence imaging: new probes from old recipes, Curr. Opin. Chem. Biol 45, 148–156. [PubMed: 29879594]

(3). Morton CL, and Houghton PJ (2007) Establishment of human tumor xenografts in immunodeficient mice, Nat. Protoc 2, 247–250. [PubMed: 17406581]

(4). Yeh HW, and Ai HW (2019) Development and Applications of Bioluminescent and Chemiluminescent Reporters and Biosensors, Annu. Rev. Anal. Chem 12, DOI: 10.1146/annurev-anchem-061318-115027.

(5). Vieira J, Pinto da Silva L, and Esteves da Silva JC (2012) Advances in the knowledge of light emission by firefly luciferin and oxyluciferin, J. Photochem. Photobiol. B 117, 33–39. [PubMed: 23026386]

(6). Haddock SH, Moline MA, and Case JF (2010) Bioluminescence in the sea, Ann. Rev. Mar. Sci 2, 443–493.

(7). Lorenz WW, McCann RO, Longiaru M, and Cormier MJ (1991) Isolation and expression of a cDNA encoding Renilla reniformis luciferase, Proc. Natl. Acad. Sci. USA 88, 4438–4442. [PubMed: 1674607]

(8). Shimomura O, Masugi T, Johnson FH, and Haneda Y (1978) Properties and reaction mechanism of the bioluminescence system of the deep-sea shrimp Oplophorus gracilorostris, Biochemistry 17, 994–998. [PubMed: 629957]

(9). Verhaegent M, and Christopoulos TK (2002) Recombinant Gaussia luciferase. Overexpression, purification, and analytical application of a bioluminescent reporter for DNA hybridization, Anal. Chem 74, 4378–4385. [PubMed: 12236345]

(10). Shimomura O, and Teranishi K (2000) Light-emitters involved in the luminescence of coelenterazine, Luminescence 15, 51–58. [PubMed: 10660666]

(11). Iwano S, Sugiyama M, Hama H, Watakabe A, Hasegawa N, Kuchimaru T, Tanaka KZ, Takahashi M, Ishida Y, Hata J, Shimozono S, Namiki K, Fukano T, Kiyama M, Okano H, Kizaka-Kondoh S, McHugh TJ, Yamamori T, Hioki H, Maki S, and Miyawaki A (2018) Single-cell bioluminescence imaging of deep tissue in freely moving animals, Science 359, 935–939. [PubMed: 29472486]

(12). Tannous BA, Kim DE, Fernandez JL, Weissleder R, and Breakefield XO (2005) Codon-optimized Gaussia luciferase cDNA for mammalian gene expression in culture and in vivo, Mol. Ther 11, 435–443. [PubMed: 15727940]

(13). Hall MP, Unch J, Binkowski BF, Valley MP, Butler BL, Wood MG, Otto P, Zimmerman K, Vidugiris G, Machleidt T, Robers MB, Benink HA, Eggers CT, Slater MR, Meisenheimer PL, Klaubert DH, Fan F, Encell LP, and Wood KV (2012) Engineered Luciferase Reporter from a Deep Sea Shrimp Utilizing a Novel Imidazopyrazinone Substrate, ACS Chem. Biol 7, 1848–1857. [PubMed: 22894855]

(14). Germain-Genevois C, Garandeau O, and Couillaud F (2016) Detection of Brain Tumors and Systemic Metastases Using NanoLuc and Fluc for Dual Reporter Imaging, Mol. Imaging Biol 18, 62–69. [PubMed: 26002233]

(15). Stacer AC, Nyati S, Moudgil P, Iyengar R, Luker KE, Rehemtulla A, and Luker GD (2013) NanoLuc reporter for dual luciferase imaging in living animals, Mol. Imaging 12, 1–13.

(16). Yeh HW, Karmach O, Ji A, Carter D, Martins-Green MM, and Ai HW (2017) Red-shifted luciferase-luciferin pairs for enhanced bioluminescence imaging, Nat. Methods 14, 971–974. [PubMed: 28869756]

(17). Chu J, Oh Y, Sens A, Ataie N, Dana H, Macklin JJ, Laviv T, Welf ES, Dean KM, Zhang F, Kim BB, Tang CT, Hu M, Baird MA, Davidson MW, Kay MA, Fiolka R, Yasuda R, Kim DS, Ng HL, and Lin MZ (2016) A bright cyan-excitable orange fluorescent protein facilitates dual-emission microscopy and enhances bioluminescence imaging in vivo, Nat Biotechnol 34, 760–767. [PubMed: 27240196]

(18). Schaub FX, Reza MS, Flaveny CA, Li W, Musicant AM, Hoxha S, Guo M, Cleveland JL, and Amelio AL (2015) Fluorophore-NanoLuc BRET Reporters Enable Sensitive In Vivo Optical Imaging and Flow Cytometry for Monitoring Tumorigenesis, Cancer Res 75, 5023–5033. [PubMed: 26424696]

(19). Suzuki K, Kimura T, Shinoda H, Bai G, Daniels MJ, Arai Y, Nakano M, and Nagai T (2016) Five colour variants of bright luminescent protein for real-time multicolour bioimaging, Nat. Commun 7, 13718. [PubMed: 27966527]

(20). Donat S, Hasenberg M, Schafer T, Ohlsen K, Gunzer M, Einsele H, Loffler J, Beilhack A, and Krappmann S (2012) Surface display of Gaussia princeps luciferase allows sensitive fungal pathogen detection during cutaneous aspergillosis, Virulence 3, 51–61. [PubMed: 22286700]

(21). Vassel N, Cox CD, Naseem R, Morse V, Evans RT, Power RL, Brancale A, Wann KT, and Campbell AK (2012) Enzymatic activity of albumin shown by coelenterazine chemiluminescence, Luminescence 27, 234–241. [PubMed: 22362656]

(22). Zhao H, Doyle TC, Wong RJ, Cao Y, Stevenson DK, Piwnica-Worms D, and Contag CH (2004) Characterization of coelenterazine analogs for measurements of Renilla luciferase activity in live cells and living animals, Mol. Imaging 3, 43–54. [PubMed: 15142411]

(23). Xiong L, Shuhendler AJ, and Rao J (2012) Self-luminescing BRET-FRET near-infrared dots for in vivo lymph-node mapping and tumour imaging, Nat. Commun 3, 1193. [PubMed: 23149738]

(24). Karlsson EA, Meliopoulos VA, Savage C, Livingston B, Mehle A, and Schultz-Cherry S (2015) Visualizing real-time influenza virus infection, transmission and protection in ferrets, Nat. Commun 6, 6378. [PubMed: 25744559]

(25). Saito K, Chang YF, Horikawa K, Hatsugai N, Higuchi Y, Hashida M, Yoshida Y, Matsuda T, Arai Y, and Nagai T (2012) Luminescent proteins for high-speed single-cell and whole-body imaging, Nat. Commun 3, 1262. [PubMed: 23232392]

(26). Tung JK, Berglund K, Gutekunst CA, Hochgeschwender U, and Gross RE (2016) Bioluminescence imaging in live cells and animals, Neurophotonics 3, 025001. [PubMed: 27226972]

(27). Tantama M, Martinez-Francois JR, Mongeon R, and Yellen G (2013) Imaging energy status in live cells with a fluorescent biosensor of the intracellular ATP-to-ADP ratio, Nat. Commun 4, 2550. [PubMed: 24096541]

(28). Fan Y, Chen Z, and Ai HW (2015) Monitoring redox dynamics in living cells with a redox-sensitive red fluorescent protein, Anal. Chem 87, 2802–2810. [PubMed: 25666702]

(29). Liu F, Song Y, and Liu D (1999) Hydrodynamics-based transfection in animals by systemic administration of plasmid DNA, Gene Ther 6, 1258–1266. [PubMed: 10455434]

(30). Kobayashi N, Nishikawa M, Hirata K, and Takakura Y (2004) Hydrodynamics-based procedure involves transient hyperpermeability in the hepatic cellular membrane: implication of a nonspecific process in efficient intracellular gene delivery, J. Gene Med 6, 584–592. [PubMed: 15133769]

(31). Zinn KR, Chaudhuri TR, Szafran AA, O'Quinn D, Weaver C, Dugger K, Lamar D, Kesterson RA, Wang X, and Frank SJ (2008) Noninvasive bioluminescence imaging in small animals, ILAR J 49, 103–115. [PubMed: 18172337]

(32). Fischer UM, Harting MT, Jimenez F, Monzon-Posadas WO, Xue HS, Savitz SI, Laine GA, and Cox CS (2009) Pulmonary Passage is a Major Obstacle for Intravenous Stem Cell Delivery: The Pulmonary First-Pass Effect, Stem Cells Dev 18, 683–691. [PubMed: 19099374]

(33). Voura EB, Jaiswal JK, Mattoussi H, and Simon SM (2004) Tracking metastatic tumor cell extravasation with quantum dot nanocrystals and fluorescence emission-scanning microscopy, Nat. Med 10, 993–998. [PubMed: 15334072]

(34). Lei Y, Tang H, Yao L, Yu R, Feng M, and Zou B (2008) Applications of mesenchymal stem cells labeled with Tat peptide conjugated quantum dots to cell tracking in mouse body, Bioconjug. Chem 19, 421–427. [PubMed: 18081241]

(35). Kalchenko V, Shivtiel S, Malina V, Lapid K, Haramati S, Lapidot T, Brill A, and Harmelin A (2006) Use of lipophilic near-infrared dye in whole-body optical imaging of hematopoietic cell homing, J. Biomed. Opt 11, 050507. [PubMed: 17092148]

(36). Edinger M, Sweeney TJ, Tucker AA, Olomu AB, Negrin RS, and Contag CH (1999) Noninvasive assessment of tumor cell proliferation in animal models, Neoplasia 1, 303–310. [PubMed: 10935484]

(37). Partlow KC, Chen J, Brant JA, Neubauer AM, Meyerrose TE, Creer MH, Nolta JA, Caruthers SD, Lanza GM, and Wickline SA (2007) 19F magnetic resonance imaging for stem/progenitor cell tracking with multiple unique perfluorocarbon nanobeacons, FASEB J 21, 1647–1654. [PubMed: 17284484]

(38). Koehne G, Doubrovin M, Doubrovina E, Zanzonico P, Gallardo HF, Ivanova A, Balatoni J, Teruya-Feldstein J, Heller G, May C, Ponomarev V, Ruan S, Finn R, Blasberg RG, Bornmann W, Riviere I, Sadelain M, O'Reilly RJ, Larson SM, and Tjuvajev JG (2003) Serial in vivo imaging of the targeted migration of human HSV-TK-transduced antigen-specific lymphocytes, Nat. Biotechnol 21, 405–413. [PubMed: 12652311]

(39). Lawrence MG, Altenburg MK, Sanford R, Willett JD, Bleasdale B, Ballou B, Wilder J, Li F, Miner JH, Berg UB, and Smithies O (2017) Permeation of macromolecules into the renal glomerular basement membrane and capture by the tubules, Proc. Natl. Acad. Sci. USA 114, 2958–2963. [PubMed: 28246329]

(40). Contag CH, Contag PR, Mullins JI, Spilman SD, Stevenson DK, and Benaron DA (1995) Photonic detection of bacterial pathogens in living hosts, Mol. Microbiol 18, 593–603. [PubMed: 8817482]

(41). Ando Y, Niwa K, Yamada N, Enomoto T, Irie T, Kubota H, Ohmiya Y, and Akiyama H (2008) Firefly bioluminescence quantum yield and colour change by pH-sensitive green emission, Nat. Photon 2, 44–47.

(42). Traut TW (1994) Physiological concentrations of purines and pyrimidines, Mol. Cell. Biochem 140, 1–22. [PubMed: 7877593]

(43). Morikofer-Zwez S, and Walter P (1989) Binding of ADP to rat liver cytosolic proteins and its influence on the ratio of free ATP/free ADP, Biochem. J 259, 117–124. [PubMed: 2497727]

(44). Meglasson MD, Nelson J, Nelson D, and Erecinska M (1989) Bioenergetic response of pancreatic islets to stimulation by fuel molecules, Metabolism 38, 1188–1195. [PubMed: 2687638]

(45). Harris DA (1996) Cellular ATP, In Principles of Medical Biology, Cell Chemistry and Physiology: Part II (Bittar EE, and Bittar N, Eds.), pp 1–47, JAI Press Inc., London, England.

(46). Veech RL, Lawson JW, Cornell NW, and Krebs HA (1979) Cytosolic phosphorylation potential, J. Biol. Chem 254, 6538–6547. [PubMed: 36399]

(47). Balaban RS, Kantor HL, Katz LA, and Briggs RW (1986) Relation between work and phosphate metabolite in the in vivo paced mammalian heart, Science 232, 1121–1123. [PubMed: 3704638]

(48). Claes F, Vodnala SK, van Reet N, Boucher N, Lunden-Miguel H, Baltz T, Goddeeris BM, Buscher P, and Rottenberg ME (2009) Bioluminescent Imaging of Trypanosoma brucei Shows Preferential Testis Dissemination Which May Hamper Drug Efficacy in Sleeping Sickness, PLOS Neglect, Trop. D 3(7), e486.

(49). Arthur Taylor JS, Antonius Plagge, Bettina Wilm, and Patricia Murray. (2018) Multicolour In Vivo Bioluminescence Imaging Using a NanoLuc-Based BRET Reporter in Combination with Firefly Luciferase, Contrast Media Mol. Imaging, 2018, 2514796. [PubMed: 30627058]

(50). Kodack DP, Chung E, Yamashita H, Incio J, Duyverman AM, Song Y, Farrar CT, Huang Y, Ager E, Kamoun W, Goel S, Snuderl M, Lussiez A, Hiddingh L, Mahmood S, Tannous BA, Eichler AF, Fukumura D, Engelman JA, and Jain RK (2012) Combined targeting of HER2 and VEGFR2 for effective treatment of HER2-amplified breast cancer brain metastases, Proc. Natl. Acad. Sci. USA 109, E3119–3127. [PubMed: 23071298]

(51). Short KR, Diavatopoulos DA, Reading PC, Brown LE, Rogers KL, Strugnell RA, and Wijburg OLC (2011) Using Bioluminescent Imaging to Investigate Synergism Between Streptococcus pneumoniae and Influenza A Virus in Infant Mice, J. Vis. Exp 50, 2357, doi: 10.3791/2357.

(52). Suda T, Gao X, Stolz DB, and Liu D (2007) Structural impact of hydrodynamic injection on mouse liver, Gene Ther 14, 129–137. [PubMed: 16988719]

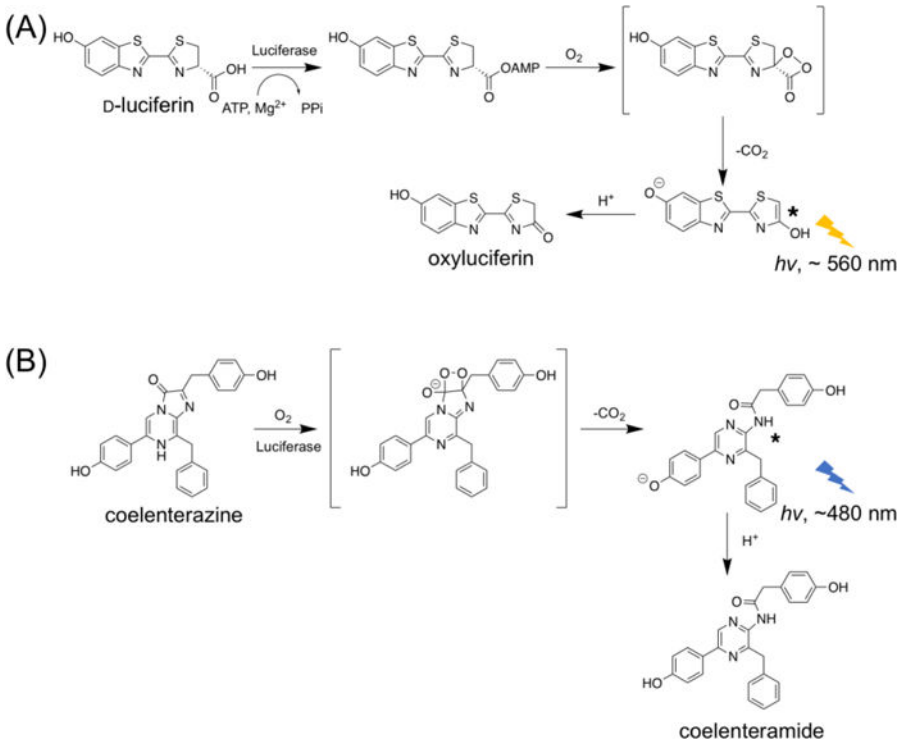

Figure 1.

Mechanisms of bioluminescence generated by luciferase-catalyzed oxidation of (**A**) D-luciferin and (**B**) coelenterazine (CTZ).

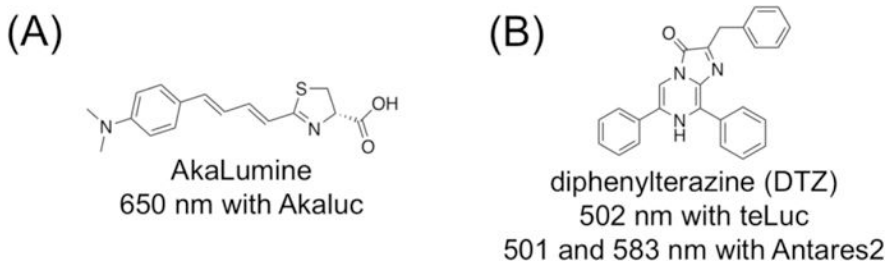

Figure 2.

Chemical structures and bioluminescence emission wavelengths of (**A**) AkaLumine and (**B**) diphenylterazine (DTZ).

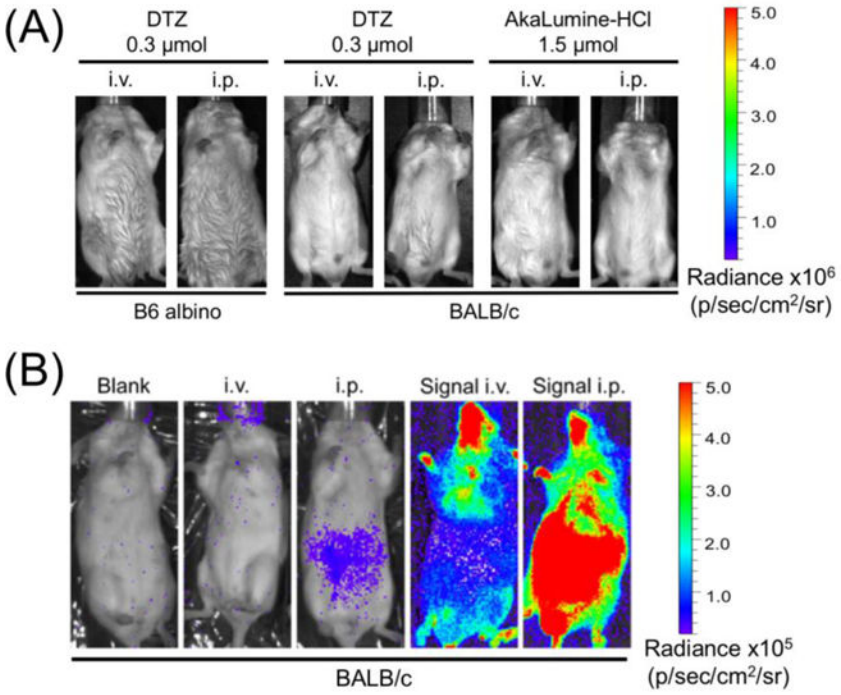

Figure 3.

(**A**) Delivery of DTZ or AkaLumine at the indicated doses via i.v. or i.p. to B6 albino mice or BALB/c mice, yielding low background. Luminescence radiance is displayed in the same scale as in Figures 4A and4**B**. (**B**) Representative bioluminescence images of BALB/c mice (from left to right: blank, i.v. injection of DTZ, i.p. injection of DTZ, and i.v. or i.p. injection of DTZ after i.v. injection of Antares2-expressing HEK 293T cells). To show the existence of background signals, luminescence radiance is displayed in a compressed scale compared to Figures 3A and4**AB**.

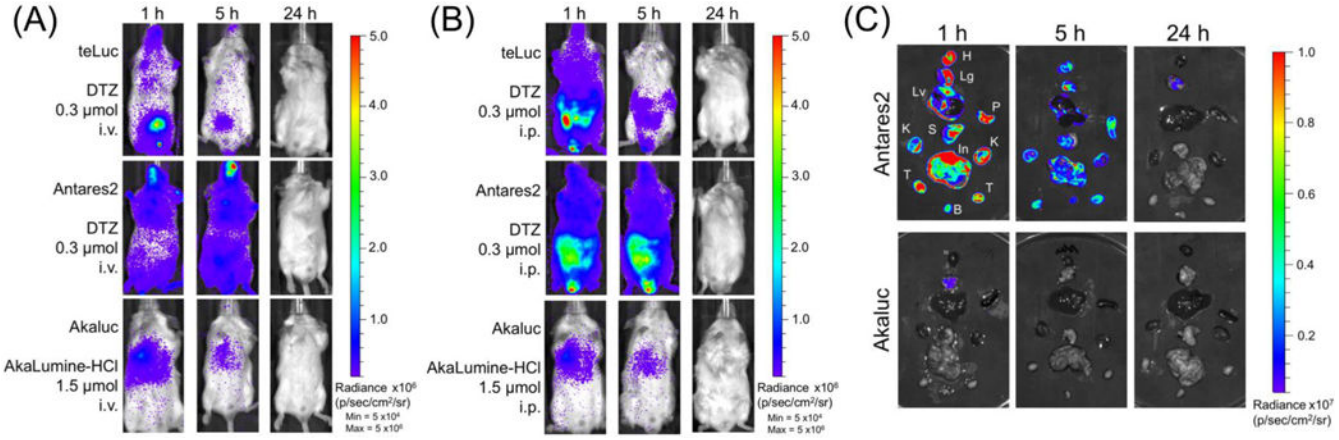

Figure 4.

(**AB**) Bioluminescence of mice post i.v. injection of 2×10^4 luciferase-labeled HEK 293T cells (three luciferase-luciferin pairs for comparison: teLuc-DTZ, Antares2-DTZ, and Akaluc-AkaLumine). BALB/c mice (n=3) were imaged 1, 5, and 24 h post injection. Luciferin substrates at indicated doses were delivered via (A) i.v. and (B) i.p., respectively. (**C**) Bioluminescence of extracted organs of mice in the Antares2-DTZ and Akaluc-AkaLumine groups from panel **B**. H: heart, Lg: lung, Lv: liver, P: spleen, S: stomach, In: intestine, K: kidney, T: testis, and B: bladder.

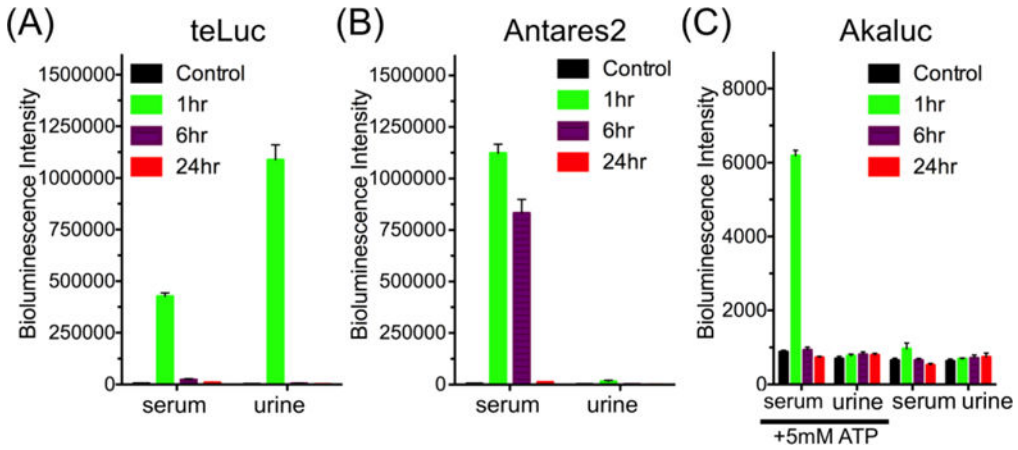

Figure 5.

Bioluminescence of serum and urine collected from mice at 1, 6, and 24 h post i.v. delivery of (**A**) teLuc-, (**B**) Antares2-, or (**C**) Akaluc-expressing HEK293T cells, suggesting that luciferases were released into blood and that the small teLuc luciferase further entered urine. Data are presented as mean and s.d. of three biological replicates. In panel C, results are shown for samples with and without supplementing ATP.

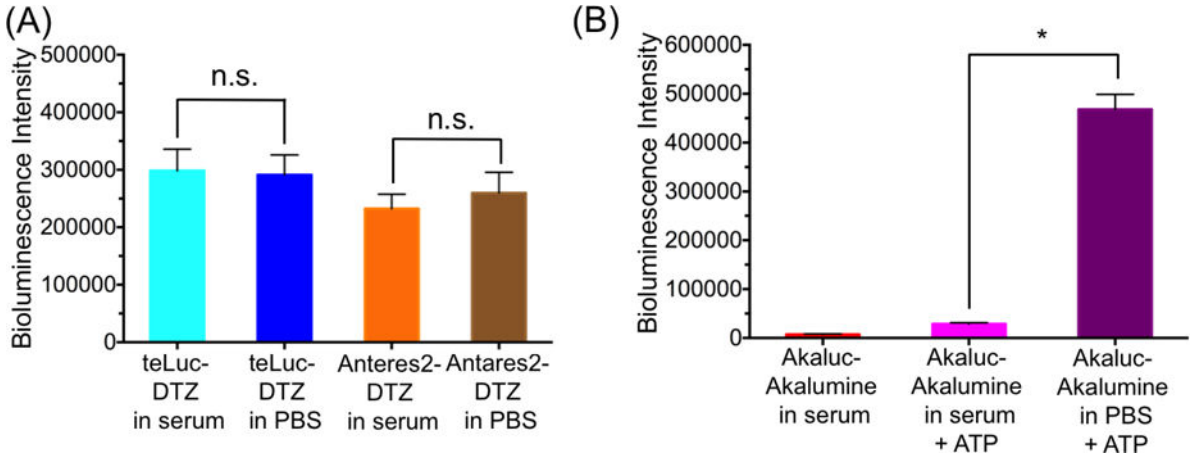

Figure 6.

(**A**) Bioluminescence intensities of purified 1 nM teLuc or Anatres2 in either PBS or mouse serum post injection of 25 μM DTZ. (**B**) Bioluminescence intensities of purified 1 μM Akaluc in PBS or mouse serum post injection of 100 μM AkaLumine with or without 5 mM ATP. *$P < 0.05$ for two-tailed t-test; n.s. not significant ($P > 0.05$).

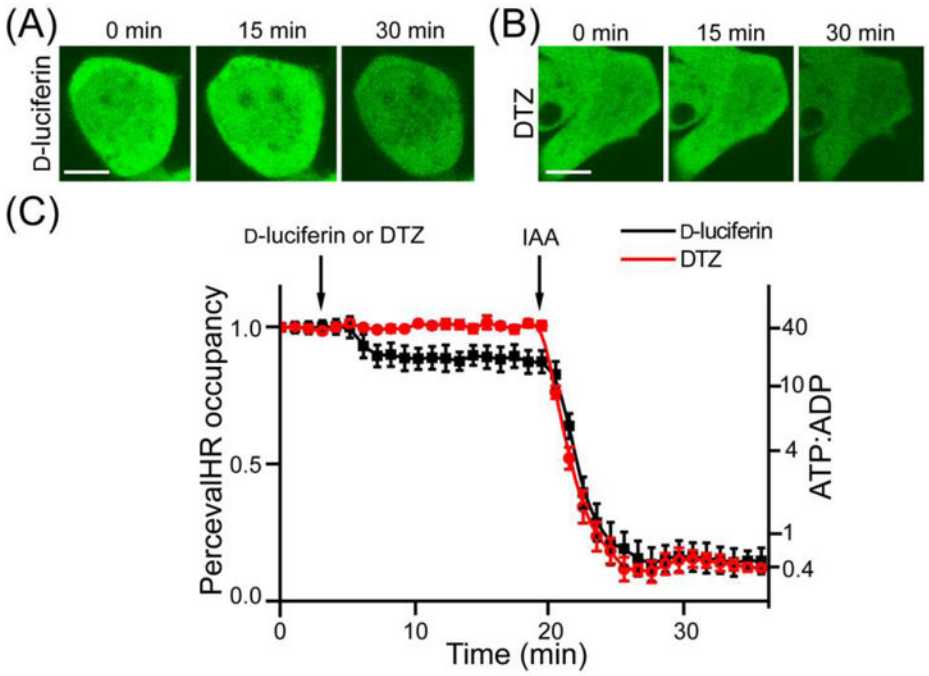

Figure 7.

(**AB**) Representative fluorescence images of HEK293T cells expressing PercevalHR and either FLuc (A) or teLuc (B), upon addition of D-luciferin (A) or DTZ (B). Iodoacetic acid (IAA) was used to treat cells after D-luciferin to completely deplete ATP. Scale bars: 10 μm. (**C**) PercevalHR occupancy and estimated ATP:ADP ratio changes upon treatment with D-luciferin or DTZ. Images were captured with 488 nm excitation, and the emission was collected from 510 to 600 nm.

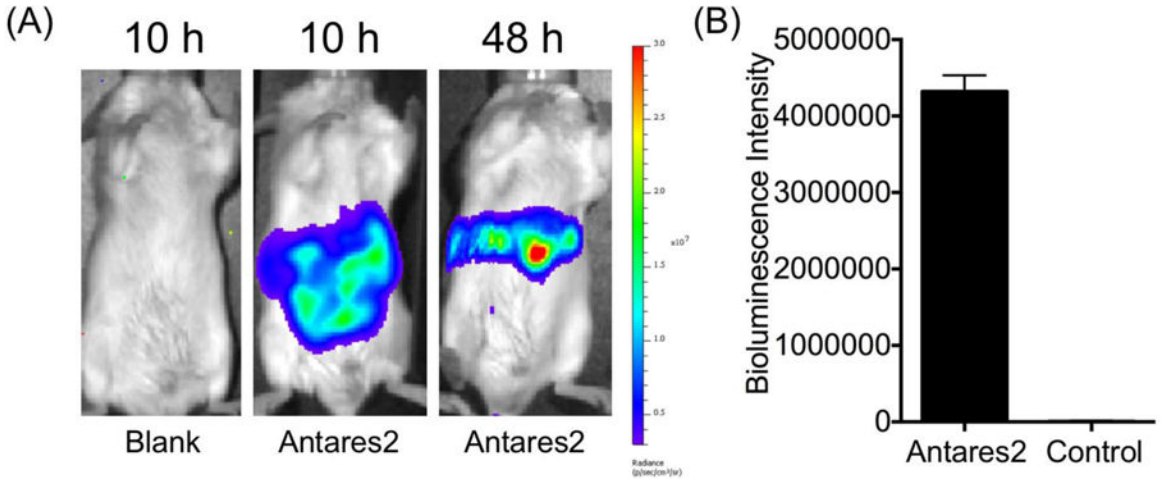

Figure 8.

(**A**) BLI of hydrodynamically transfected mice at 10 h and 48 h post transfection. An empty pcDNA3 plasmid was used for control mice and pcDNA3-Antareas2 was used to derive Antareas2-positive mice. (**B**) Quantification of bioluminescence of serum isolated from mice at 10 h post hydrodynamic transfection (n=3).

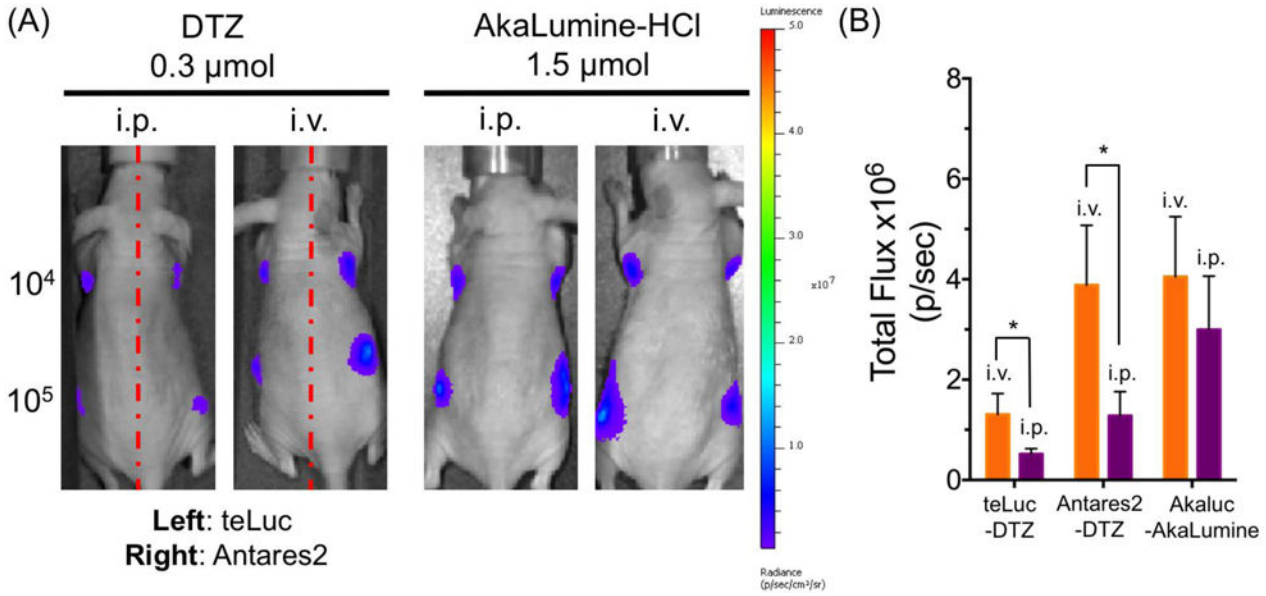

Figure 9.

BLI of mice with xenograft tumors. (**A**) BLI (n = 4) on day 5 post injection of 10^4 or 10^5 luciferase-expressing HeLa cells to the left and right dorsolateral thoracolumbar regions of NU/J mice. Substrates were administered via either i.v. or i.p. administration. (**B**) Quantitative analysis of bioluminescence intensity of sites inoculated with 10^5 cells. Data are presented as mean and s.d. of four biological replicates. $*P < 0.05$ for two-tailed *t*-test.